JCTC Journal of Chemical Theory and Computation

Article

pubs.acs.org/JCTC

Assessment of Tuning Methods for Enforcing Approximate Energy Linearity in Range-Separated Hybrid Functionals

Jonathan D. Gledhill,[†] Michael J. G. Peach,[‡] and David J. Tozer[†,*]

[†]Department of Chemistry, Durham University, South Road, Durham, DH1 3LE, United Kingdom

[‡]Department of Chemistry, Faraday Building, Lancaster University, Lancaster, LA1 4YB, United Kingdom

Supporting Information

ABSTRACT: A range of tuning methods, for enforcing approximate energy linearity through a system-by-system optimization of a range-separated hybrid functional, are assessed. For a series of atoms, the accuracy of the frontier orbital energies, ionization potentials, electron affinities, and orbital energy gaps is quantified, and particular attention is paid to the extent to which approximate energy linearity is actually achieved. The tuning methods can yield significantly improved orbital energies and orbital energy gaps, compared to those from conventional functionals. For systems with integer M electrons, optimal results are obtained using a tuning norm based on the highest occupied orbital energy of the M and $M + 1$ electron systems, with deviations of just 0.1−0.2 eV in these quantities, compared to exact values. However, detailed examination for the carbon atom illustrates a subtle cancellation between errors arising from nonlinearity and errors in the computed ionization potentials and electron affinities used in the tuning.

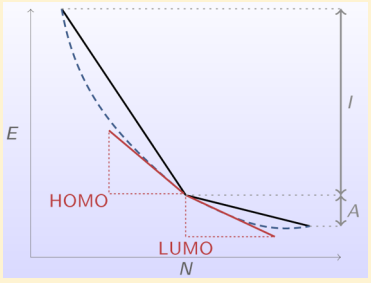

1. INTRODUCTION

A significant problem in Kohn−Sham density functional theory[1] (DFT) is the delocalization error,[2−4] present in commonly used exchange−correlation functionals. This problem underlies many of the well-known failures of approximate DFT, including the underestimation of quantities such as reaction barrier heights,[5] band gaps,[6] energies of dissociating molecular ions,[2,3,7,8] and charge−transfer excitation energies.[9]

Delocalization error can be illustrated by considering the variation in the total electronic energy, E, as a function of electron number, N. Perdew et al.[10] showed that the exact E varies linearly with fractional N, with discontinuities in the gradient $\partial E/\partial N$ at integer N. The overall E vs N behavior is therefore a piecewise function comprising a series of linear segments between the integers. Functionals that suffer from delocalization error do not exhibit this piecewise linear behavior—instead, they give a convex deviation from linearity, such that the energy at fractional N is too low. As a result, these functionals favor locally fractional charge, overdelocalizing systems and underestimating their energy. Such deviation from linearity is also known as many-electron self-interaction error.[11−16]

This erroneous nonlinear behavior has important implications for the Kohn−Sham orbital energies and their relationship to ionization potentials and electron affinities. Let M be an integer and $0 < f < 1$. The piecewise linearity of the exact E vs N curve implies that for a system with $N = M - f$ electrons, the exact $\partial E/\partial N$ is equal to the negative of the exact vertical ionization potential of the M-electron system, denoted I_0^M, independent of the value of f. Similarly, for a system with $N = M + f$ electrons, $\partial E/\partial N$ equals the negative of the exact vertical electron affinity of the M-electron system, denoted A_0^M, again independent of f. From Janak's theorem,[17] $\partial E/\partial N$ equals the energy of the Kohn−Sham orbital whose occupation is varying. It follows that

$$\varepsilon_M(M - f) = -I_0^M \tag{1}$$

$$\varepsilon_{M+1}(M + f) = -A_0^M \tag{2}$$

where $\varepsilon_M(M - f)$ is the energy of the Mth orbital of the $M - f$ electron system and $\varepsilon_{M+1}(M + f)$ is the energy of the $(M + 1)$th orbital of the $M + f$ electron system. In the limit $f \to 0$, eqs 1 and 2 can be identified as the exact Koopmans relationships

$$\varepsilon_H^{M,-} = -I_0^M \tag{3}$$

$$\varepsilon_L^{M,+} = -A_0^M \tag{4}$$

where $\varepsilon_H^{M,-}$ and $\varepsilon_L^{M,+}$ are the exact highest-occupied (HOMO) and lowest-unoccupied (LUMO) molecular orbital energies of the M-electron system, determined on the $f \to 0$ electron-deficient and electron-abundant sides of the integer, respectively. The use of the $\pm$ superscript to denote the side of the integer is vital, because the exact exchange−correlation potential jumps discontinuously as the integer is crossed, meaning a given orbital energy also jumps by the same amount. In practical calculations, using approximate exchange−correlation functionals within the usual generalized Kohn−Sham approach,[18] $\partial E/\partial N$ is again equal to the orbital energy[6] and so the value of $\partial E/\partial N$ on the $f \to 0$ electron-deficient and electron-abundant sides of the integer M equals the HOMO energy, ε_H^M, and the LUMO energy, ε_L^M, of the M-electron

Received: July 8, 2013
Published: August 22, 2013

system, respectively. However, the incorrect E vs N curvature associated with the delocalization error means that $\varepsilon_H^M \gg -I_0^M$ and $\varepsilon_L^M \ll -A_0^M$ (refs 6 and 19).

Several approaches can be used to impose near-linear E vs N behavior. Vydrov et al.[12] demonstrated that many electron self-interaction error was significantly reduced by applying a self-interaction correction;[20] see also refs 21−23. The MCY3 and rCAM-B3LYP functionals[14] were specifically designed to achieve near-linear behavior and they have shown some success.[24] Zheng et al.[25] proposed a nonempirical scaling correction to largely restore linearity, which was later extended[26] to properly account for orbital relaxation effects. Very recently, Kraisler and Kronik[27] demonstrated that the exact Koopmans ionization relationship could be largely restored using an ensemble treatment. A more pragmatic approach is to simply tune the proportion of exact orbital exchange in global[28−30] or range-separated[31−38] hybrid functionals on a system-by-system basis, in order to approximately recover Koopmans or other conditions, which are necessary (but not sufficient) for linearity. The success of this approach reflects the fact that Hartree−Fock theory typically yields concave E vs N curves, and so, the inclusion of exact orbital exchange tends to cancel the incorrect convex behavior. Karolewski et al.[39] recently highlighted a number of caveats for such an approach, most notably the violation of size-consistency. The aim of the present study is to provide a systematic investigation of a wide range of tuning methods, quantifying the accuracy of Koopmans relationships, ionization potentials, electron affinities, and orbital energy gaps. Particular attention is paid to the degree of linearity of the resulting E vs N curves. Results and conclusions are presented in Sections 2 and 3, respectively.

2. RESULTS

2.1. Choice of Tuning Methods. Figure 1 illustrates the key quantities in the context of an E vs N diagram. The dashed blue curve represents the convex behavior of a typical approximate exchange−correlation functional within the generalized Kohn−Sham approach. The slopes of this curve on the limiting electron-deficient side of the M- and $(M+1)$-electron integer systems are the HOMO energies of those systems, ε_H^M and ε_H^{M+1}, respectively. The slopes on the limiting electron-abundant side of the $(M-1)$- and M-electron systems are the LUMO energies of those systems, ε_L^{M-1} and ε_L^M, respectively. Also indicated are the vertical ionization potentials, I^M and I^{M+1}, and electron affinities, A^{M-1} and A^M, of the integer systems, determined as the differences between the energies of the integer systems, calculated using the same approximate functional. The solid black curve indicates a linear interpolation between the integer energies, which will more closely resemble the shape of the exact curve because approximate functionals tend to perform more accurately at integer electron-number. For brevity, we denote the E vs N curve from $M-1 \rightarrow M$ as the left-hand side (LHS) and the curve from $M \rightarrow M+1$ as the right-hand side (RHS).

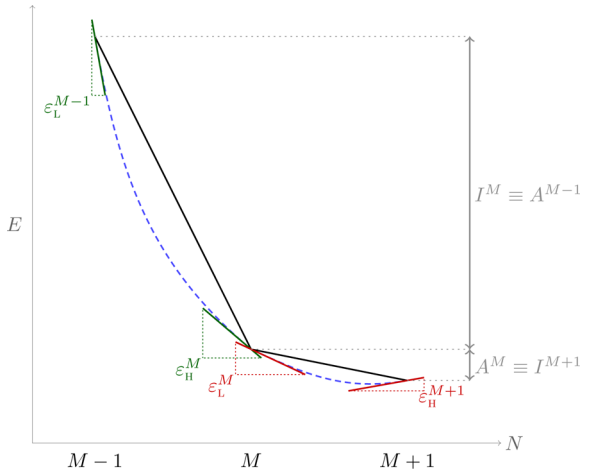

Figure 1. Schematic representation of the quantities involved in the tuning methods.

In the context of Figure 1, the aim of a tuning method is to make the nonlinear blue curve more closely resemble the piecewise linear black one. If this could be achieved on the LHS then the following condition would hold,

$$\varepsilon_H^M = \varepsilon_L^{M-1} = -I^M = -A^{M-1} \tag{5}$$

which suggests three possible tuning criteria:

$$\varepsilon_H^M = -I^M \tag{6}$$

$$\varepsilon_L^{M-1} = -A^{M-1} \tag{7}$$

and

$$\varepsilon_H^M = \varepsilon_L^{M-1} \tag{8}$$

where the former two conditions have been expressed as Koopmans-type relationships. For each of these criteria, a tuning approach can be defined as a minimization, on a system-by-system basis, of a norm measuring the extent to which that condition is satisfied. The norms based on the three tuning criteria above are denoted

$$H_{LHS} = |\varepsilon_H^M + I^M| \tag{9}$$

$$L_{LHS} = |\varepsilon_L^{M-1} + A^{M-1}| \tag{10}$$

$$\Omega_{LHS} = |\varepsilon_L^{M-1} - \varepsilon_H^M| \tag{11}$$

respectively. We can similarly define the RHS analogues,

$$H_{RHS} = |\varepsilon_H^{M+1} + I^{M+1}| \tag{12}$$

$$L_{RHS} = |\varepsilon_L^M + A^M| \tag{13}$$

$$\Omega_{RHS} = |\varepsilon_L^M - \varepsilon_H^{M+1}| \tag{14}$$

In both cases, H and L refer to the Koopmans conditions appropriate to the given E vs N segment, while Ω gives an indication of the degree of E vs N curvature. It is worth noting that tuning to H or L constrains the orbital energies to be close to the *calculated* ionization potential or electron affinity but says nothing about how well they reproduce the exact quantities. Similarly, tuning to Ω constrains the two orbital energies/slopes to be equal to each other but not necessarily equal to the correct value. We shall investigate both of these issues in the present study.

By choosing one of the above minimization criteria, one attempts to impose linearity on a single E vs N segment. Baer and co-workers, however, noted[32,38] that in order to obtain an accurate estimation of properties such as the fundamental gap, $I_0^M - A_0^M$, as a difference of Kohn−Sham orbital energies, *both* segments needed to be accurately described. To achieve this,

Table 1. Mean Absolute Deviations (in eV) in Various Quantities, Over All Atoms, Relative to Exact Reference Values,[57] for Conventional Functionals and Each Tuning Norm

	ε_H^M	ε_L^M	I^M	A^M	Ω_{LHS}	Ω_{RHS}	$\varepsilon_L^M - \varepsilon_H^M$
Conventional Functionals							
PBE	4.10	3.04	0.15	0.19	8.22	5.71	7.13
B3LYP	3.16	2.35	0.17	0.17	6.57	4.37	5.50
BNL	0.76	0.33	0.15	0.32	1.46	0.50	0.85
LC-B3LYP	0.36	0.37	0.26	0.24	1.29	0.31	0.62
Single-Segment Tuning							
H_{LHS}	0.26	0.33	0.26	0.17	0.16	0.79	0.53
L_{LHS}	0.34	0.40	0.25	0.16	0.17	0.91	0.68
Ω_{LHS}	0.30	0.37	0.26	0.17	0.09	0.85	0.61
H_{RHS}	0.63	0.42	0.26	0.23	1.82	0.21	0.92
L_{RHS}	0.30	0.22	0.26	0.21	1.16	0.21	0.39
Ω_{RHS}	0.46	0.32	0.25	0.23	1.45	0.04	0.65
Double-Segment Tuning							
$\|\|J_{H,H}\|\|_1$	0.24	0.32	0.26	0.17	0.19	0.78	0.51
$\|\|J_{H,H}\|\|_2$	0.09	0.21	0.26	0.19	0.64	0.49	0.19
$\|\|J_{H,H}\|\|_3$	0.10	0.20	0.26	0.19	0.71	0.45	0.17
$\|\|J_{H,H}\|\|_4$	0.11	0.20	0.27	0.19	0.73	0.44	0.16
$\|\|J_{H,L}\|\|_1$	0.25	0.32	0.26	0.17	0.18	0.78	0.52
$\|\|J_{H,L}\|\|_2$	0.17	0.26	0.26	0.18	0.37	0.65	0.34
$\|\|J_{H,L}\|\|_3$	0.16	0.24	0.26	0.18	0.42	0.62	0.31
$\|\|J_{H,L}\|\|_4$	0.14	0.23	0.27	0.18	0.45	0.61	0.28
$\|\|J_{L,H}\|\|_1$	0.33	0.39	0.25	0.16	0.16	0.89	0.67
$\|\|J_{L,H}\|\|_2$	0.11	0.22	0.26	0.19	0.55	0.55	0.22
$\|\|J_{L,H}\|\|_3$	0.11	0.20	0.26	0.19	0.61	0.51	0.19
$\|\|J_{L,H}\|\|_4$	0.11	0.20	0.26	0.19	0.64	0.50	0.17
$\|\|J_{L,L}\|\|_1$	0.34	0.40	0.25	0.16	0.17	0.90	0.67
$\|\|J_{L,L}\|\|_2$	0.22	0.29	0.26	0.18	0.26	0.72	0.44
$\|\|J_{L,L}\|\|_3$	0.19	0.27	0.26	0.18	0.33	0.68	0.38
$\|\|J_{L,L}\|\|_4$	0.18	0.26	0.26	0.18	0.35	0.67	0.37
reference value	$-I_0^M$	$-A_0^M$	I_0^M	A_0^M	0	0	$I_0^M - A_0^M$

they introduced two new tuning norms, which in our notation are written

$$J_{H,L} = H_{LHS} + L_{RHS} \tag{15}$$

and

$$J_{H,H} = H_{LHS} + H_{RHS} \tag{16}$$

By analogy, we can also define

$$J_{L,H} = L_{LHS} + H_{RHS} \tag{17}$$

$$J_{L,L} = L_{LHS} + L_{RHS} \tag{18}$$

A similar form for the tuning norm has also been proposed,[35,38] differing from eq 16 only in the cross-terms of its square, which we write as

$$\|J_{H,H}\|_2 = \sqrt{H_{LHS}^2 + H_{RHS}^2} \tag{20}$$

and for which we can also consider the related combinations $\|J_{H,L}\|_2$, $\|J_{L,H}\|_2$, and $\|J_{L,L}\|_2$. Indeed, we observe that eqs 16 and 20 are the first two terms of a series of p-norms,

$$\|J_{H,H}\|_p = \sqrt[p]{H_{LHS}^p + H_{RHS}^p} \tag{21}$$

which leads us to consider the general p-norm

$$\|J_{x,y}\|_p = \sqrt[p]{x^p + y^p} \tag{22}$$

where x and y refer to LHS and RHS conditions, respectively; we consider up to $p = 4$. Overall, this leads to a total of 22 tuning norms, listed in Table 1.

2.2. Assessment of Tuning Methods. We considered the same set of atoms as Baer and co-workers,[32,38] comprising Li−F, Na−Cl, and Ga−Br. The quantity M in the tuning norms is the number of electrons in the neutral atom. The ground state spin configuration was used for both neutral atoms and ions. Tuning was carried out using a range-separated[40−47] form of B3LYP,[48−52] denoted LC-B3LYP using the notation of ref 43, with the fraction of exact exchange varying from 0 to 100% (i.e., $\alpha = 0$, $\beta = 1$) at a rate defined by the range-separation parameter μ. For each atom, calculations were performed using a series of μ values, and the value that minimized each norm, denoted μ^*, was determined to 2 d.p. For comparison, calculations were also carried out using a representative GGA (PBE[53]), a conventional hybrid functional (B3LYP) and nontuned range-separated hybrids (BNL[47,54] and LC-B3LYP, each with range-separation parameter $\mu = 0.4\ a_0^{-1}$). Calculations were performed using the Gaussian 09[55] and CADPAC[56] programs, with the aug-cc-pVTZ basis set.

Inevitably, use of these tuning methods increases the computational effort, since calculations must be performed over a range of μ values. In the present study—where multiple criteria are investigated, each with a (potentially) different minimum—we used a coarse grid of μ values, refining as necessary close to the minima. For a single tuning norm, the procedure could be carried out more efficiently but would still

dx.doi.org/10.1021/ct400592a | J. Chem. Theory Comput. 2013, 9, 4414−4420

Table 2. Deviations (in eV) in Various Quantities, For the Carbon Atom, Relative to Exact Reference Values,[59] for Each Tuning Norm[a]

	μ^*	ε_H^M	ε_L^M	I^M	A^M	Ω_{LHS}	Ω_{RHS}	$\varepsilon_L^M-\varepsilon_H^M$
				Single-Segment Tuning				
H_{LHS}	0.66	−0.47	0.57	0.46	−0.03	−0.05	1.44	1.03
L_{LHS}	0.68	−0.52	0.61	0.45	−0.05	0.05	1.50	1.12
Ω_{LHS}	0.67	−0.49	0.59	0.45	−0.04	0.00	1.47	1.08
H_{RHS}	0.36	0.89	−0.50	0.44	0.21	−2.75	−0.31	−1.38
L_{RHS}	0.43	0.44	−0.14	0.46	0.15	−1.87	0.29	−0.57
Ω_{RHS}	0.39	0.68	−0.33	0.45	0.18	−2.35	−0.03	−1.01
				Double-Segment Tuning				
$\|\|J_{H,H}\|\|_1$	0.65	−0.44	0.55	0.46	−0.03	−0.11	1.41	0.99
$\|\|J_{H,H}\|\|_2$	0.53	−0.04	0.24	0.47	0.06	−0.91	0.91	0.29
$\|\|J_{H,H}\|\|_3$	0.52	0.00	0.21	0.47	0.07	−1.00	0.86	0.21
$\|\|J_{H,H}\|\|_4$	0.51	0.04	0.18	0.47	0.08	−1.08	0.81	0.14
reference value		$-I_0^M$	$-A_0^M$	I_0^M	A_0^M	0	0	$I_0^M-A_0^M$

[a] μ^* is the optimal range-separation parameter (in a_0^{-1}).

require a number of separate calculations (typically greater than 20).

We assess the tuning methods in several ways. To test the Koopmans relationships, we consider the deviation of ε_H^M and ε_L^M from the exact $-I_0^M$ and $-A_0^M$, respectively;[57] it is also pertinent to consider the deviation of the calculated I^M and A^M (determined from integer energy differences) from I_0^M and A_0^M. The quantities Ω_{LHS} and Ω_{RHS} provide a measure of linearity for the individual segments, and so, we consider the deviation of these quantities from zero (by construction, Ω will be near-zero when it is successfully employed as the tuning norm, but this will not necessarily be the case for a general tuning norm). Finally, we consider the deviation of $\varepsilon_L^M-\varepsilon_H^M$ from the fundamental gap $I_0^M - A_0^M$. Mean absolute deviations are presented in Table 1, determined by calculating individual absolute deviations for each atom using its corresponding μ^* value and then averaging over the set of atoms. The corresponding standard deviations are presented in the Supporting Information. For clarity, the results are divided into those determined using conventional functionals and those determined using tuned functionals with single-segment (H, L, and Ω) and double-segment (J) tuning.

2.2.1. Conventional Functionals. First, consider the results in Table 1 determined using the PBE functional. As expected, the values of ε_H^M and ε_L^M differ significantly from $-I_0^M$ and $-A_0^M$, by 3 to 4 eV. By contrast, the directly computed I^M and A^M are more than an order of magnitude more accurate. The large values of 6 to 8 eV for the linearity measures Ω_{LHS} and Ω_{RHS} quantify the significant E vs N curvature. As noted in Section 1, the errors in ε_H^M and ε_L^M are of opposite sign and so the deviation is amplified when the difference is used to compute the gap. It follows that the gaps $\varepsilon_L^M - \varepsilon_H^M$ deviate by more than 7 eV from $I_0^M - A_0^M$. In the case of a GGA such as PBE, the difference between the fundamental gap and the associated orbital energy gap is approximately equal to the exact exchange−correlation integer discontinuity;[10,19] the relationship between curvature and integer discontinuity has recently been discussed by Stein et al.[58]

B3LYP performs slightly better than PBE for each of the problematic quantities, reflecting the reduction in convexity caused by the addition of some exact exchange, while maintaining the low deviations in I^M and A^M. The nontuned range-separated hybrids BNL and LC-B3LYP show a further marked improvement in the problematic quantities, although the deviations remain non-negligible. With these two functionals, the I^M and A^M values degrade marginally.

2.2.2. Single-Segment Tuning. Next, consider the functionals tuned to criteria on a single E vs N segment, using H, L, or Ω as tuning norms. The deviations in ε_H^M and ε_L^M are generally close to those from the nontuned range-separated functionals. The lowest deviations in ε_H^M and ε_L^M are, not surprisingly, obtained by tuning to H_{LHS} and L_{RHS}, respectively, since these explicitly optimize the Koopmans conditions that are being assessed. Importantly, these deviations are still nonzero, challenging the assumption that simply tuning to the calculated I^M or A^M is sufficient—one must also consider the quality of the calculated I^M or A^M itself, that is, how accurate the relative energies of the integer-electron systems are. In fact, I^M is in virtually constant deviation by 0.25 eV whichever tuning is used, and—somewhat counterintuitively—A^M is slightly better when tuning the LHS rather than the RHS.

Tuning to H_{LHS} and L_{LHS} gives comparatively low values of Ω_{LHS}, up to five times smaller than Ω_{RHS}, indicating that the tuning is relatively successful at linearizing the LHS segment, but at the expense of the RHS. Tuning to H_{RHS} and L_{RHS} yields analogous behavior, with Ω_{RHS} values up to nine times smaller than Ω_{LHS}. When used as tuning norms, Ω_{LHS} and Ω_{RHS} give, by construction, near-zero values for their respective linearity measures (although large values are seen on the nonoptimized side). However, all that a small value of Ω indicates is that the slopes at the two integers are essentially the same—not necessarily that they are equal to the correct value. In fact, the discrepancy between the deviations in ε_H^M and ε_L^M and those in the calculated I^M and A^M confirms that the slopes are not correct; see Section 2.3.

For both LHS and RHS tuning norms, the deviations in the gap $\varepsilon_L^M - \varepsilon_H^M$ are of a similar magnitude to the nontuned range-separated functionals. The lowest deviations are obtained when tuning to H_{LHS} and L_{RHS}, reflecting the fact that these two conditions individually yield the most accurate ε_H^M and ε_L^M, respectively, which are the two components of the gap.

2.2.3. Double-Segment Tuning. Next consider the functionals tuned to criteria on both E vs N segments, using the various J in eq 22 as tuning norms. In all cases, the deviations in ε_H^M and ε_L^M reduce notably from $p = 1$ to $p = 2$, with little subsequent change for $p > 2$; the best results are obtained using the $\|J_{H,H}\|_p$ series, with deviations as small as 0.1 to 0.2 eV. However, similar trends are not seen in the computed I^M and

dx.doi.org/10.1021/ct400592a | J. Chem. Theory Comput. 2013, 9, 4414−4420

A^M—the deviation in I^M is an almost constant 0.26 eV on average, for all of the tuning norms tested. This has obvious implications for the tuning methods, which rely on attempting to constrain the frontier orbital energies to these incorrect I^M values.

As p increases beyond unity, Ω_{LHS} increases, which is somewhat counterintuitive given that $\varepsilon_{\mathrm{H}}^M$ improves. A more intuitive trend is observed for Ω_{RHS}, which reduces as $\varepsilon_{\mathrm{L}}^M$ improves. Despite yielding the most accurate $\varepsilon_{\mathrm{H}}^M$ and $\varepsilon_{\mathrm{L}}^M$, the values of Ω_{LHS} and Ω_{RHS} are both significant for the $\|J_{\mathrm{H,H}}\|_p$ series with $p > 1$, indicating that substantial nonlinearity remains. Insight into these observations is provided in Section 2.3.

The accuracy of the gaps $\varepsilon_{\mathrm{L}}^M - \varepsilon_{\mathrm{H}}^M$ again reflect the accuracy of the orbital energies: the best results are obtained for the $\|J_{\mathrm{H,H}}\|_p$ series, with deviations reducing to less than 0.2 eV.

2.3. Representative System: The Carbon Atom. Further insight into the behavior of the tuned functionals is obtained by focusing on a single atom, thereby allowing the quantities in Table 1 to be explicitly related to an E vs N curve. We consider the carbon atom with $M = 6$ and $5 \leqslant N \leqslant 7$. Table 2 presents μ^* values determined for the carbon atom, using selected tuning norms, along with the deviations (calculated minus reference) in $\varepsilon_{\mathrm{H}}^M$, $\varepsilon_{\mathrm{L}}^M$, I^M, A^M, Ω_{LHS}, Ω_{RHS}, and $\varepsilon_{\mathrm{L}}^M - \varepsilon_{\mathrm{H}}^M$, computed using μ^*. The dependence of these quantities on the choice of tuning norm largely follows the behavior of the average quantities in Table 1.

For each tuning norm in Table 2, an E vs N curve was produced by fixing μ at the corresponding value of μ^* and smoothly varying the number of α electrons from 3 to 5, with the number of β electrons fixed at 2. To most effectively illustrate the nonlinearity of the E vs N curve, we plot the deviation of the calculated energy from a linear interpolation between the calculated energies at integer N; we will refer to these curves as E vs N deviation curves. By construction, the interpolated and calculated energies agree at integer. For noninteger values, a horizontal line along zero indicates a linear E vs N curve, while a positive/negative deviation indicates a concave/convex curve. Results are presented in Figures 2−4.

A pair of straight lines is superimposed onto each E vs N deviation curve, one on the electron-deficient side and one on the electron-abundant side of $N = 6$. These lines are the differences between the *exact* piecewise curve and the linear interpolation between calculated integers, aligned at $N = 6$. The slopes of the lines indicate the limiting slopes that an E vs N deviation curve would have to exhibit at $N = 6$, in order to yield $\varepsilon_{\mathrm{H}}^M = -I_0^M$ and $\varepsilon_{\mathrm{L}}^M = -A_0^M$, respectively. We term them 'exact slopes' in the context of an E vs N deviation plot. These exact slopes provide a useful guide to the quality of a functional: the difference between the slope of the E vs N deviation curve and the exact slope quantifies the deviations in $\varepsilon_{\mathrm{H}}^M$ and $\varepsilon_{\mathrm{L}}^M$ from $-I_0^M$ and $-A_0^M$, while the deviation of the exact slope from a horizontal line quantifies the deviations in I^M and A^M, again from I_0^M and A_0^M. We note that if the exact slope is not horizontal then satisfaction of the exact Koopmans conditions ($\varepsilon_{\mathrm{H}}^M = -I_0^M$; $\varepsilon_{\mathrm{L}}^M = -A_0^M$) will *require* nonlinearity in the E vs N curve.

Figure 2 presents the E vs N deviation curves for the three μ^* values determined by tuning to the RHS. The three μ^* values are rather different from one another and so the E vs N behavior of each is also quite different. In moving from H_{RHS} to Ω_{RHS} to L_{RHS}, the slopes on either side of $N = 6$ move closer to the exact slopes, and so, the deviations in $\varepsilon_{\mathrm{H}}^M$ and $\varepsilon_{\mathrm{L}}^M$ in Table 2 reduce. The exact slopes are notably offset from horizontal, reflecting the deviations in I^M and A^M in Table 2. By construction, tuning to H_{RHS} and L_{RHS} yields—for the RHS segment—near-zero slopes at $N = 7$ and $N = 6$, respectively. However, in both cases the unconstrained end of the RHS segment exhibits a much larger slope, leading to the small but non-negligible Ω_{RHS} values in Table 2; by contrast the LHS segment is highly convex, with large Ω_{LHS} values. By construction, tuning to Ω_{RHS} yields essentially identical slopes at $N = 6$ and $N = 7$ for the RHS segment and hence near-zero values for Ω_{RHS}, but the slopes themselves are not zero, resulting in a curve with a point of inflection. The LHS segment is again highly convex, with a correspondingly large Ω_{LHS} value.

Figure 3 shows the analogous curves when tuning to the LHS. The three μ^* values are now very close to one another and so the differences in the E vs N behavior are much less pronounced. The near-linearity of the LHS is much more pronounced than the RHS was in Figure 2 and so, at first sight, one might expect an accurate $\varepsilon_{\mathrm{H}}^M$. However, the plot simply illustrates that $\varepsilon_{\mathrm{H}}^M \approx -I^M$; by contrast the deviation of the exact slope from horizontal indicates that $I^M \neq I_0^M$ and so the

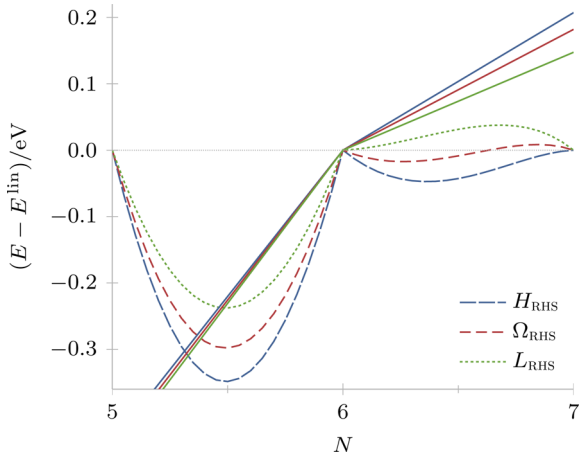

Figure 2. E vs N deviation curves (dashed/dotted curves) and exact slopes (solid straight lines) for the carbon atom using RHS tuning norms. See text for definitions of these quantities.

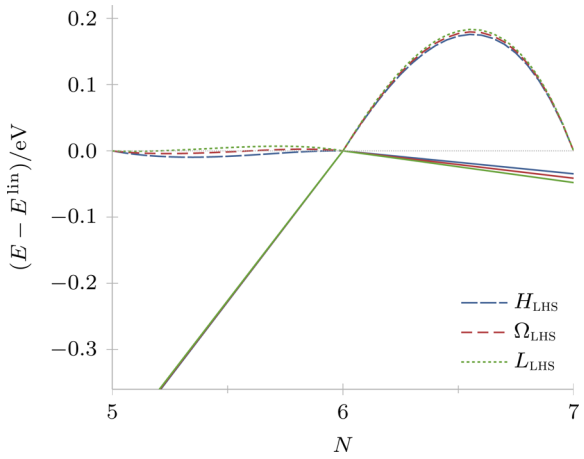

Figure 3. E vs N deviation curves (dashed/dotted curves) and exact slopes (solid straight lines) for the carbon atom using LHS tuning norms. See text for definitions of these quantities.

dx.doi.org/10.1021/ct400592a | J. Chem. Theory Comput. 2013, 9, 4414−4420

discrepancy between ε_H^M and $-I_0^M$ is actually significant. The deviation in ε_L^M is of a similar magnitude—in this case, the deviation arises largely due to the curvature, rather than the error in A^M, which is now much smaller.

Finally, consider the curves obtained by tuning to both segments. Each set of p-norms shows a similar trend, so we choose the most successful method, $\|J_{H,H}\|_p$, to illustrate the behavior. Figure 4 presents the E vs N deviation curves for the

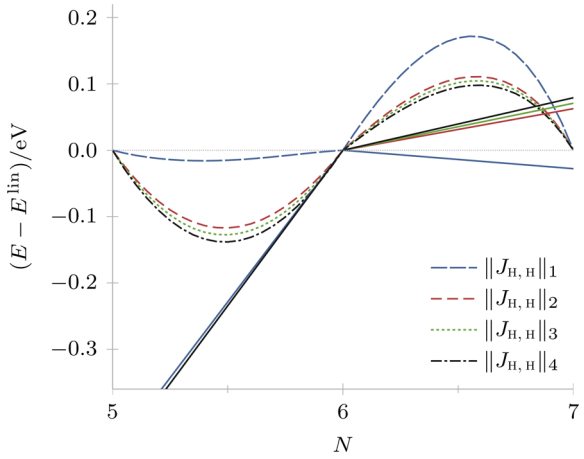

Figure 4. E vs N deviation curves (dashed/dotted curves) and exact slopes (solid straight lines) for the carbon atom using double-segment tuning norms. See text for definitions of these quantities.

μ^* values obtained for $1 \leqslant p \leqslant 4$. When $p = 1$, $\mu^* = 0.65$, which is essentially the same as the value obtained when tuning to the LHS segment, and so, the curve is close to those in Figure 3. Increasing p to 2 yields $\mu^* = 0.53$, roughly midway between the LHS-only and RHS-only optimized values. This results in some reduction in concavity on the RHS (Ω_{RHS} in Table 2 decreases) but increased convexity on the LHS (Ω_{LHS} increases in magnitude), so that neither side shows near-linear behavior. As p is increased to 3 and 4, μ^* decreases marginally again, with a further small shift in the E vs N deviation curves. Despite the lack of linearity on either side, using $p > 1$ yields slopes that are closest to the exact slopes, and hence, the values of ε_H^M and ε_L^M are optimal. The good performance of the $p > 1$ functionals therefore arises from a convenient error cancellation between lack of linearity and errors in I^M and A^M.

3. CONCLUSIONS

We have assessed a range of tuning methods for enforcing approximate energy linearity, that is, reducing delocalization error, through a system-by-system optimization of a range-separated hybrid functional. For a series of atoms, the accuracy of frontier orbital energies, ionization potentials, electron affinities, and orbital energy gaps has been quantified, and particular attention has been paid to the extent to which approximate linearity is actually achieved in the resulting E vs N curve.

The tuning approaches can yield significantly improved orbital energies and orbital energy gaps, compared to those from conventional functionals. For M-electron systems, optimal results were obtained using a tuning norm based on the HOMO energy of the M and $M + 1$ electron systems, with deviations of just 0.1 to 0.2 eV in these quantities, compared to exact values. However, detailed examination for the carbon atom illustrates a subtle cancellation between errors arising from nonlinearity and errors in the computed ionization potentials and electron affinities used in the tuning.

■ ASSOCIATED CONTENT

Ⓢ Supporting Information

Standard deviations corresponding to the data in Table 1 and E vs N curves corresponding to the data in Figures 2−4. This material is available free of charge via the Internet at http://pubs.acs.org.

■ AUTHOR INFORMATION

Corresponding Author

*E-mail: d.j.tozer@durham.ac.uk.

Notes

The authors declare no competing financial interest.

■ ACKNOWLEDGMENTS

The authors thank the EPSRC for financial support.

■ REFERENCES

(1) Kohn, W.; Sham, L. J. *Phys. Rev.* **1965**, *140*, A1133−A1138.
(2) Mori-Sánchez, P.; Cohen, A. J.; Yang, W. *J. Chem. Phys.* **2006**, *125*, 201102.
(3) Ruzsinszky, A.; Perdew, J. P.; Csonka, G. I.; Vydrov, O. A.; Scuseria, G. E. *J. Chem. Phys.* **2007**, *126*, 104102.
(4) Cohen, A. J.; Mori-Sánchez, P.; Yang, W. *Science* **2008**, *321*, 792−794.
(5) Johnson, B. G.; Gonzales, C. A.; Gill, P. M.; Pople, J. A. *Chem. Phys. Lett.* **1994**, *221*, 100−108.
(6) Cohen, A. J.; Mori-Sánchez, P.; Yang, W. *Phys. Rev. B* **2008**, *77*, 115123.
(7) Bally, T.; Sastry, G. N. *J. Phys. Chem. A* **1997**, *101*, 7923−7925.
(8) Xie, Y.; Schaefer, H. F.; Fu, X.-Y.; Liu, R.-Z. *J. Chem. Phys.* **1999**, *111*, 2532.
(9) Tozer, D. J. *J. Chem. Phys.* **2003**, *119*, 12697−12699.
(10) Perdew, J. P.; Parr, R. G.; Levy, M.; Balduz, J. L. *Phys. Rev. Lett.* **1982**, *49*, 1691−1694.
(11) Haunschild, R.; Henderson, T. M.; Jiménez-Hoyos, C. A.; Scuseria, G. E. *J. Chem. Phys.* **2010**, *133*, 134116.
(12) Vydrov, O. A.; Scuseria, G. E.; Perdew, J. P. *J. Chem. Phys.* **2007**, *126*, 154109.
(13) Ruzsinszky, A.; Perdew, J. P.; Csonka, G. I.; Vydrov, O. A.; Scuseria, G. E. *J. Chem. Phys.* **2006**, *125*, 194112.
(14) Cohen, A. J.; Mori-Sanchez, P.; Yang, W. *J. Chem. Phys.* **2007**, *126*, 191109.
(15) Dutoi, A. D.; Head-Gordon, M. *Chem. Phys. Lett.* **2006**, *422*, 230−233.
(16) Zhang, Y.; Yang, W. *J. Chem. Phys.* **1998**, *109*, 2604−2608.
(17) Janak, J. *Phys. Rev. B* **1978**, *18*, 7165−7168.
(18) Seidl, A.; Görling, A.; Vogl, P.; Majewski, J.; Levy, M. *Phys. Rev. B* **1996**, *53*, 3764−3774.
(19) Teale, A. M.; De Proft, F.; Tozer, D. J. *J. Chem. Phys.* **2008**, *129*, 44110.
(20) Perdew, J. P.; Zunger, A. *Phys. Rev. B* **1981**, *23*, 5048−5079.
(21) Vydrov, O. A.; Scuseria, G. E.; Perdew, J. P.; Ruzsinszky, A.; Csonka, G. I. *J. Chem. Phys.* **2006**, *124*, 094108.
(22) Körzdörfer, T.; Kümmel, S.; Mundt, M. *J. Chem. Phys.* **2008**, *129*, 014110.
(23) Hofmann, D.; Kümmel, S. *Phys. Rev. B* **2012**, *86*, 201109.
(24) Heaton-Burgess, T.; Yang, W. *J. Chem. Phys.* **2010**, *132*, 234113.
(25) Zheng, X.; Cohen, A. J.; Mori-Sánchez, P.; Hu, X.; Yang, W. *Phys. Rev. Lett.* **2011**, *107*, 026403.
(26) Zheng, X.; Zhou, T.; Yang, W. *J. Chem. Phys.* **2013**, *138*, 174105.
(27) Kraisler, E.; Kronik, L. *Phys. Rev. Lett.* **2013**, *110*, 126403.
(28) Rios-Font, R.; Sodupe, M.; Rodríguez-Santiago, L.; Taylor, P. R. *J. Phys. Chem. A* **2010**, *114*, 10857−10863.

(29) Vydrov, O. A.; Scuseria, G. E. *J. Chem. Phys.* **2006**, *125*, 234109.
(30) Dumont, E.; Laurent, A. D.; Assfeld, X.; Jacquemin, D. *Chem. Phys. Lett.* **2011**, *501*, 245−251.
(31) Salzner, U.; Baer, R. *J. Chem. Phys.* **2009**, *131*, 231101.
(32) Stein, T.; Eisenberg, H.; Kronik, L.; Baer, R. *Phys. Rev. Lett.* **2010**, *105*, 266802.
(33) Stein, T.; Kronik, L.; Baer, R. *J. Am. Chem. Soc.* **2009**, *131*, 2818−2820.
(34) Stein, T.; Kronik, L.; Baer, R. *J. Chem. Phys.* **2009**, *131*, 244119.
(35) Kuritz, N.; Stein, T.; Baer, R.; Kronik, L. *J. Chem. Theory Comput.* **2011**, *7*, 2408−2415.
(36) Refaely-Abramson, S.; Baer, R.; Kronik, L. *Phys. Rev. B* **2011**, *84*, 075144.
(37) Minami, T.; Nakano, M.; Castet, F. *J. Phys. Chem. Lett.* **2011**, *2*, 1725−1730.
(38) Kronik, L.; Stein, T.; Refaely-Abramson, S.; Baer, R. *J. Chem. Theory Comput.* **2012**, *8*, 1515−1531.
(39) Karolewski, A.; Kronik, L.; Kümmel, S. *J. Chem. Phys.* **2013**, *138*, 204115.
(40) Gill, P. M. W.; Adamson, R. D.; Pople, J. A. *Mol. Phys.* **1996**, *88*, 1005−1010.
(41) Leininger, T.; Stoll, H.; Werner, H.-J.; Savin, A. *Chem. Phys. Lett.* **1997**, *275*, 151−160.
(42) Iikura, H.; Tsuneda, T.; Yanai, T.; Hirao, K. *J. Chem. Phys.* **2001**, *115*, 3540−3544.
(43) Yanai, T.; Tew, D. P.; Handy, N. C. *Chem. Phys. Lett.* **2004**, *393*, 51−57.
(44) Vydrov, O. A.; Heyd, J.; Krukau, A. V.; Scuseria, G. E. *J. Chem. Phys.* **2006**, *125*, 74106.
(45) Chai, J.-D.; Head-Gordon, M. *J. Chem. Phys.* **2008**, *128*, 84106.
(46) Rohrdanz, M. A.; Martins, K. M.; Herbert, J. M. *J. Chem. Phys.* **2009**, *130*, 54112.
(47) Livshits, E.; Baer, R. *Phys. Chem. Chem. Phys.* **2007**, *9*, 2932−41.
(48) Becke, A. D. *Phys. Rev. A* **1988**, *38*, 3098−3100.
(49) Becke, A. D. *J. Chem. Phys.* **1993**, *98*, 5648−5652.
(50) Stephens, P. J.; Devlin, F. J.; Chabalowski, C. F.; Frisch, M. J. *J. Phys. Chem.* **1994**, *98*, 11623−11627.
(51) Lee, C.; Yang, W.; Parr, R. G. *Phys. Rev. B* **1988**, *37*, 785−789.
(52) Vosko, S. H.; Wilk, L.; Nusair, M. *Can. J. Phys.* **1980**, *58*, 1200−1211.
(53) Perdew, J. P.; Burke, K.; Ernzerhof, M. *Phys. Rev. Lett.* **1996**, *77*, 3865−3868.
(54) Baer, R.; Neuhauser, D. *Phys. Rev. Lett.* **2005**, *94*, 43002.
(55) Frisch, M. J.; Trucks, G. W.; Schlegel, H. B.; Scuseria, G. E.; Robb, M. A.; Cheeseman, J. R.; Scalmani, G.; Barone, V.; Mennucci, B.; Petersson, G. A.; Nakatsuji, H.; Caricato, M.; Li, X.; Hratchian, H. P.; Izmaylov, A. F.; Bloino, J.; Zheng, G.; Sonnenberg, J. L.; Hada, M.; Ehara, M.; Toyota, K.; Fukuda, R.; Hasegawa, J.; Ishida, M.; Nakajima, T.; Honda, Y.; Kitao, O.; Nakai, H.; Vreven, T.; Montgomery Jr., J. A.; Peralta, J. E.; Ogliaro, F.; Bearpark, M.; Heyd, J. J.; Brothers, E.; Kudin, K. N.; Staroverov, V. N.; Kobayashi, R.; Normand, J.; Raghavachari, K.; Rendell, A.; Burant, J. C.; Iyengar, S. S.; Tomasi, J.; Cossi, M.; Rega, N.; Millam, J. M.; Klene, M.; Knox, J. E.; Cross, J. B.; Bakken, V.; Adamo, C.; Jaramillo, J.; Gomperts, R.; Stratmann, R. E.; Yazyev, O.; Austin, A. J.; Cammi, R.; Pomelli, C.; Ochterski, J. W.; Martin, R. L.; Morokuma, K.; Zakrzewski, V. G.; Voth, G. A.; Salvador, P.; Dannenberg, J. J.; Dapprich, S.; Daniels, A. D.; Farkas, O.; Foresman, J. B.; Ortiz, J. V.; Cioslowski, J.; Fox, D. J. *Gaussian 09* Revision A.02; Gaussian Inc.: Wallingford, CT, 2009.
(56) Amos, R. D.; Alberts, I. L.; Andrews, J. S.; Cohen, A. J.; Colwell, S. M.; Handy, N. C.; Jayatilaka, D.; Knowles, P. J.; Kobayashi, R.; Laming, G. J.; Lee, A. M.; Maslen, P. E.; Murray, C. W.; Palmieri, P.; Rice, J. E.; Simandiras, E. D.; Stone, A. J.; Su, M.-D.; Tozer, D. J. *CADPAC 6.5, The Cambridge Analytic Derivatives Package*; Cambridge University: Cambridge, U.K., 1998.
(57) Values for I_0^M and A_0^M were obtained from the second and third columns of the table in the Appendix of ref 59, with the exception of the electron affinity of As, where a more recent value of 0.8048 eV was taken from ref 60, and the electron affinity of N, where the ground state value of zero was used.
(58) Stein, T.; Autschbach, J.; Govind, N.; Kronik, L.; Baer, R. *J. Phys. Chem. Lett.* **2012**, *3*, 3740−3744.
(59) Cardenas, C.; Ayers, P.; De Proft, F.; Tozer, D. J.; Geerlings, P. *Phys. Chem. Chem. Phys.* **2011**, *13*, 2285−2293.
(60) Haynes, W. M.; Lide, D. R. *CRC Handbook of Chemistry and Physics*, 92nd ed.; CRC Press: Boca Raton, FL, 2012.